Supplemental Information

A High-Efficiency and Stable Organic Solar Cell with Balanced Crystallization Kinetics

Weichao Zhang, Yaochang Yue, Rongsheng Yang, Yingyu Zhang, Wenna Du, Guanghao Lu, Jianqi Zhang, Huiqiong Zhou, Xuning Zhang,* Yuan Zhang**

Materials

PM6, BTP-eC9, Y6-1O and $PC_{71}BM$ were purchased from Solarmer Company. PEDOT:PSS (Baytron Clevios P VP AI 4083, Germany) was obtained from Heraeus Group. All reagents were purchased from Sigma-Aldrich, Acros, Alfa Aesar or TCI and used as received.

UV-Vis absorption and PL spectroscopic measurements

Absorption and Fluorescence spectra of donor polymers and acceptors in solid thin films were fabricated by spin-coating their solutions in chloroform atop the quartz glass substrates. The pure donor film and the pure acceptor film were spin-coated from a chloroform solution of 10 mg/ml. All the blend films were fabricated under the optimal conditions for preparations of optimal solar cells. The absorption spectrum was measured on a Hitachi U-3010 UV-visible spectrophotometer, and the fluorescence detection was performed on a Hitachi F-7000 spectrophotometer.

Device fabrications and measurements

All solar cells were prepared using a conventional structure of ITO/PEDOT:PSS/active layer/PNDIT-F3N-Br/Ag. Indium tin oxide (ITO) coated glass substrates were pre-cleaned with detergent, deionized water, CMOS grade acetone and isopropanol in turn for 20 minutes, The substrates were dried by nitrogen gas and then treated by UV-Ozone for 20 min before use. PEDOT:PSS was spin-coated onto the cleaned ITO substrates at 4000 rpm for 30 s, then the substrates were moved to oven and dried at 165 °C for 10 min. Next, the substrate was transferred to a glove box in nitrogen atmosphere. Blends of PM6:BTP-eC9 (wt. ratio = 1:1.2), PM6:Y6-1O (wt. ratio = 1:1.2), PM6:BTP-eC9:Y6-1O (wt. ratio = 1:1.2:0.1), PM6:BTP-eC9:$PC_{71}BM$ (wt. ratio = 1:1.2:0.1), PM6:BTP-eC9:Y6-1O:$PC_{71}BM$ (wt. ratio = 1:1.2:0.1:0.1) were dissolved in chloroform (CF) at a total concentration of 17.8 mg/mL, respectively.

The active layer solution was magnetically stirred on a hot plate at 40 ℃ for 2-2.5 hours. Half an hour prior to spin coating the active layer solution, 0.5 vol% of 1,8-diiodooctane was added. The active layer solution was spin-coated on PEDOT:PSS at 4000 rpm/min for 30 s and then thermally annealed at 100 °C. Floowing that, the PNDIT-F3N-Br solution (1 mg/mL) was spin-coated to form the electron transporting layer. Finally, a 100 nm of Ag electrode was evaporated. The effective area of the device was 4 mm^2. An AM 1.5G simulated solar illumination (AAA grade, XES-70S1) was used as the light source. The illumination intensity in front of the cell sample was calibrated to be 100 mW/cm^2 with a reference silicon cell. The EQE measurements were performed with the as-fabricated solar cell using a QE-R3011 instrument (Enli Technology Co. Ltd., Taiwan).

Charge carrier mobility determination

The hole-only and electron-only the electron-only devices were fabricated with a configuration of ITO/ZnO/active layer/PDINO/Ag and hole-only devices were in configuration of ITO/PEDOT:PSS/active layer/Au. The corresponding charge mobility was extracted by fitting the current density versus voltage curves using the Mott-Gurney law[1,2] ($J = 9\varepsilon_r\varepsilon_0\mu V^2/8L^3$, where J is the current density, ε_r is the dielectric permittivity of the active layer, ε_0 is the vacuum permittivity, L is the thickness of the active layer, μ is the hole or electron mobility, and V equals V_{app} - V_{bi}, with V_{app} being the applied potential, and V_{bi} the built-in potential. From the plot of $J^{1/2}$ versus V, the hole and electron mobilities were deduced. The film thickness was obtained by using a step profiler (KLA-Tencor, D-120).

Transient absorption spectroscopy (TAS)

For TAS measurements, a Ti:Sapphire femtosecond laser system provided laser pulses for the femtosecond transient absorption measurements. A regenerative amplifier (Spectra Physics, Spitfire) seeded with a mode-locked Ti: sapphire laser (Spectra Physics, Tsunami) delivered laser pulses at 800 nm (120 fs, 1 kHz), which were then divided into two components by using a 9:1 beam splitter. The major component was sent to an optical parametric amplifier (Spectra Physics, OPA-800CF) to generate the pump pulses (760 & 840 nm, 130 fs, 1 kHz). The minor component was further attenuated and focused into a 3-mm sapphire plate to generate the probe pulses. A short-pass filter (SPF-750, CVI) was inserted into the probe beam to select visible probe (420-750 nm). The time delay between the pump and probe beams was regulated through a computer-controlled motorized translation stage in the pump beam. The temporal resolution between the pump and the

probe pulses was determined to be 150 fs (FWHM). The transmitted light was detected by a CMOS linear image sensor. The excitation pulsed energy was ~ 50 nJ/pulse as measured at the sample site. The stability of the samples was spectrophotometrically checked before and after each experiment. Analysis of the kinetic traces derived from time-resolved spectra was performed using nonlinear least-square fitting to a general sum-of-exponentials function after deconvolution of instrument response function (IRF). All the spectroscopic measurements were carried out at room temperature.

GIWAXS and AFM measurements

2D GIWAXS measurements were performed based on a Xeuss SAXS/WAXS beamline system at the National Center for Nanoscience and Technology, China. Samples were prepared on Si substrates under the same conditions as those used for device fabrication. AFM measurement was performed by using a Bruker Dimension icon in tapping mode. All film samples were spin-cast on the ITO/PEDOT:PSS substrates under the same conditions as those used for device fabrication.

In-situ optical spectroscopy

In-situ UV-vis absorption spectrum was performed on a home-made in-situ optical spectroscopic system using the transmission (T) mode. The light source and detector were positioned precisely above and below the substrate, respectively, and on the same vertical line. The detector collected the transmission spectra ranging from 400 to 1000 nm during the spinning the substrate (or chuck). The UV-vis absorption spectra were calculated from the transmission spectra according to the equation $\Delta\lambda = -\log(T)$, where is the absorbance at a certain wavelength (λ) and T is the calculated transmittance. The light source and detector were turned on before coating the film, so time zero refers to the point when the first solution transmission spectrum was collected by the detector. Before time zero, there was only noise in the transmission spectra.

In-situ photoluminescence spectra were collected by using a laser (MGL-III-532nm-300m W-BH80018) with a temporal resolution of 0.1 s. The excitation wavelength was 485 nm. The light source and detector were fixed above the film and signals were collected upon spin-coating the solution onto the quartz substrate.

EQE_{EL} and high-sensitivity EQE measurements

EQE_{EL} measurements were performed using a home-built setup using a Keithley 2400 to inject current to the solar cells. Emission photon-flux from the solar cells was recorded using a Si detector (Hamamatsu s1337-

1010BQ) and a Keithley 6482 picoammeter. The FTPS-EQE measurement was carried out on an Enlitech FTPS PECT-600 instrument.

Transient photocurrent and photovoltage measurements

Transient photocurrent (TPC) and photovoltage (TPV) measurements were performed on a home-made transient system and the photovoltage/photocurrent decay dynamics were recorded on a digital oscilloscope (Tektronix MDO4104C). Voltages at open circuit and currents under short circuit conditions were measured over a 1 MΩ and a 50 Ω resistor, respectively.

Surface energy characterization

Contact angle measurements were performed (at room temperature) on a Drop Shape Analyzer (DSA100, KRÜSS) in the static mode. The surface free energy of each film was calculated through fitting. Specifically, the contact angle, averaged from the left and right angles of a sessile drop, was measured using the tangential method in the KRÜSS software. Deionized water and diiodomethane (1.5 μL) were dropped onto SiO2 wafers with the neat film, and the droplet was photographed after reaching equilibrium at the gas-liquid-solid interface. The contact angle was fixed within a standard deviation of ±1°. The Flory-Huggins interaction parameter was calculated using the relation, $\chi_{da}=K(\sqrt{\gamma_d}-\sqrt{\gamma_a})$.

Solid-state ^{19}FMAS NMR (magic angle spinning nuclear magnetic microscopy)

Solid-state ^{19}F MAS NMR spectra were recorded on a Bruker AVANCE III 400 solid-state NMR Spectrometer with a 2.5mm H-F-X Probe. The spinning speed was at 20 kHz. A recycle delay time of 1s was selected. The ^{19}F chemical shift was referenced to KF at -133.40 ppm.

Supporting figures and tables

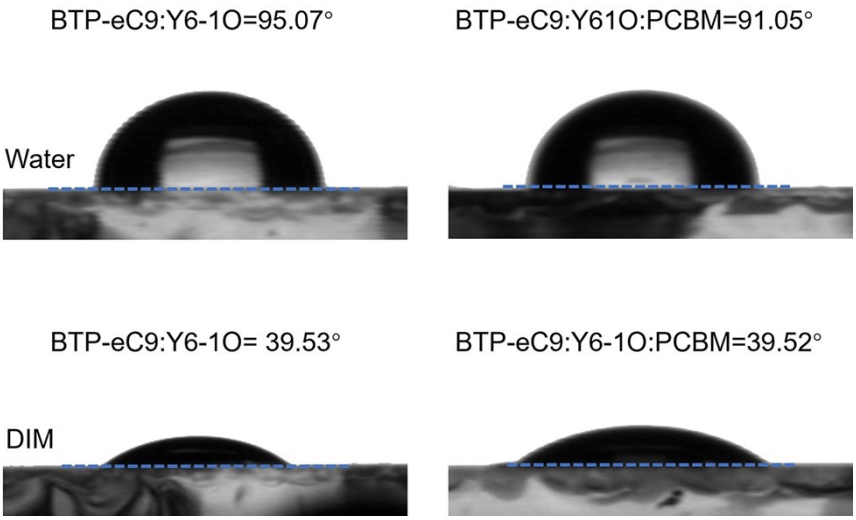

Figure S1. Snapshots of water and DIM droplets on the top surfaces of different blend films.

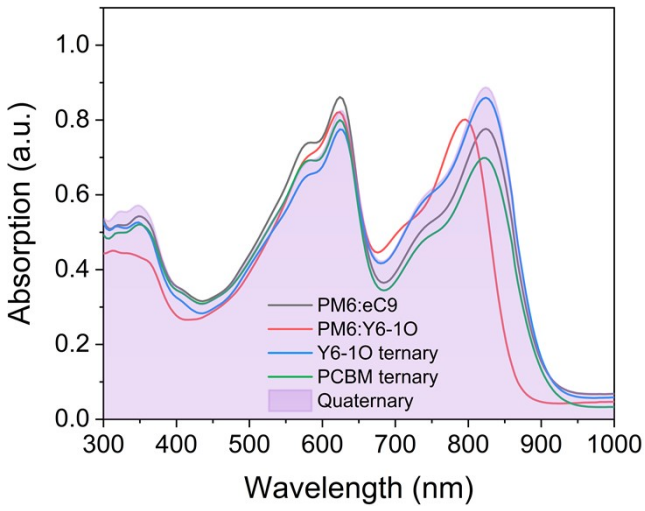

Figure S2. Normalized absorption spectra of various BHJ films.

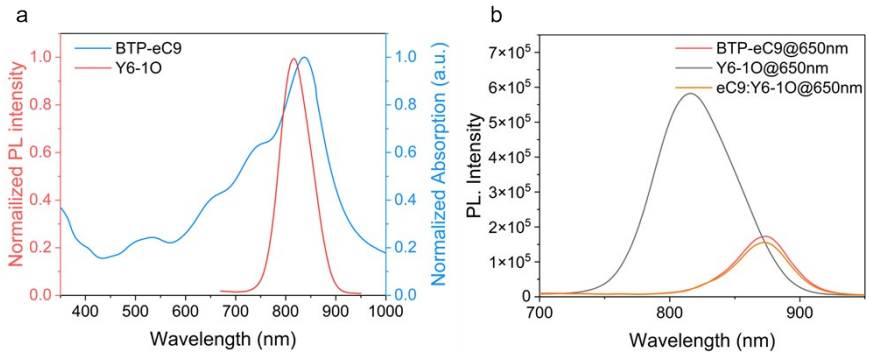

Figure S3. (a) Normalized photoluminescence (PL) spectra of the BTP-eC9 film and normalized UV-Vis absorption spectra of the Y6-1O film. (b) Photoluminescence spectra of the BTP-eC9 and Y6-1O and BTP-eC9:Y6-1O blend film. The excitation wavelength is 650 nm.

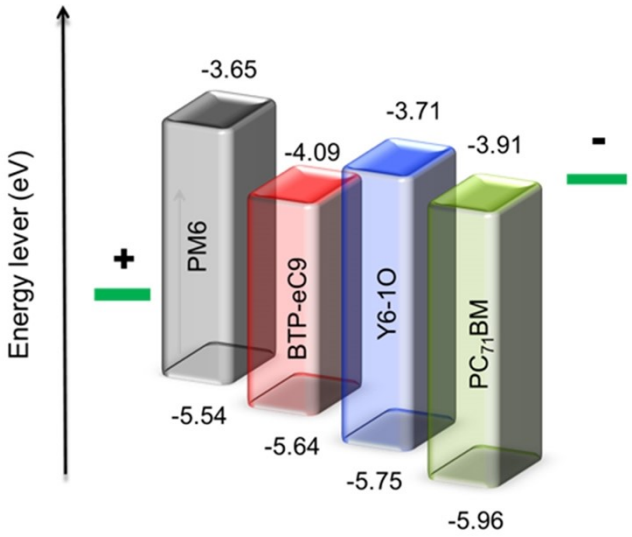

Figure S4. Sketched energy levels of PM6 donor and different acceptors used in this study.

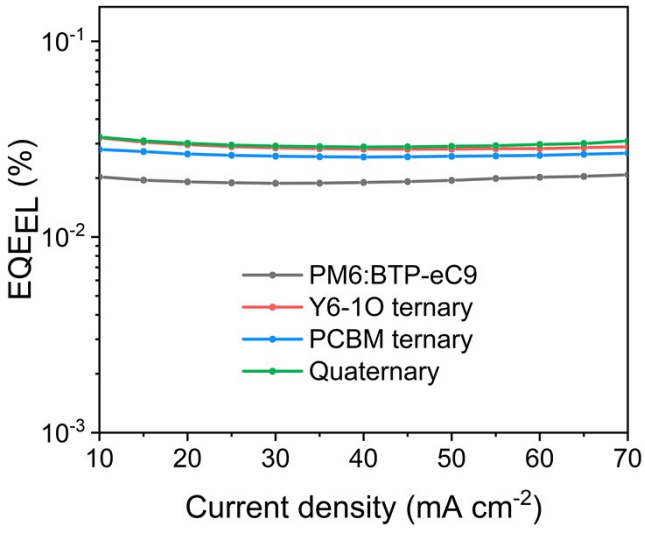

Figure S5. EL quantum efficiencies as a function of injected current density determined on various OSCs.

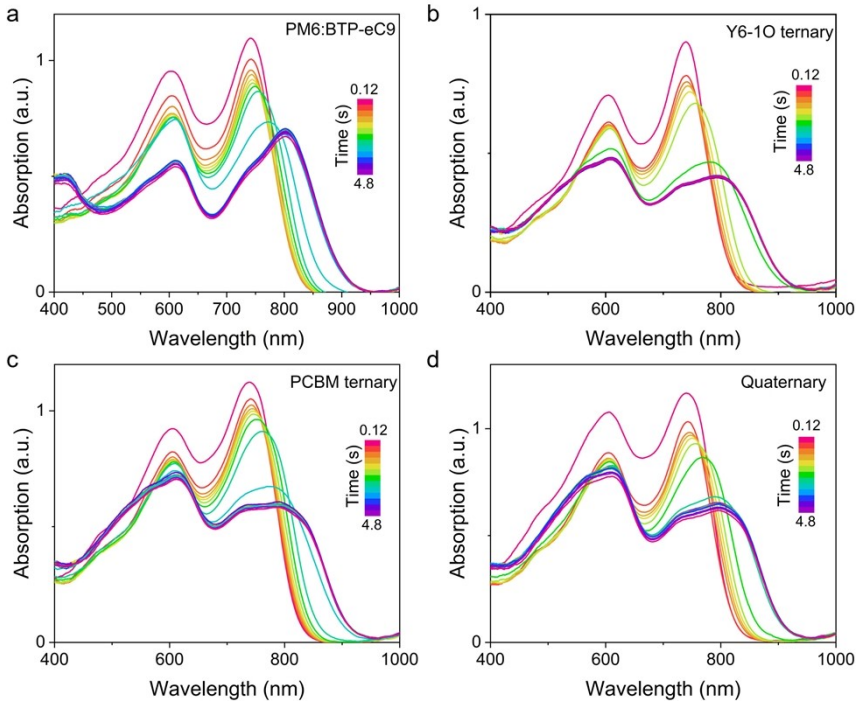

Figure S6. *In-situ* UV-vis absorption spectra of (a) PM6:BTP-eC9, (b) Y6-1O ternary, (c) PCBM ternary and (d) quaternary blend films.

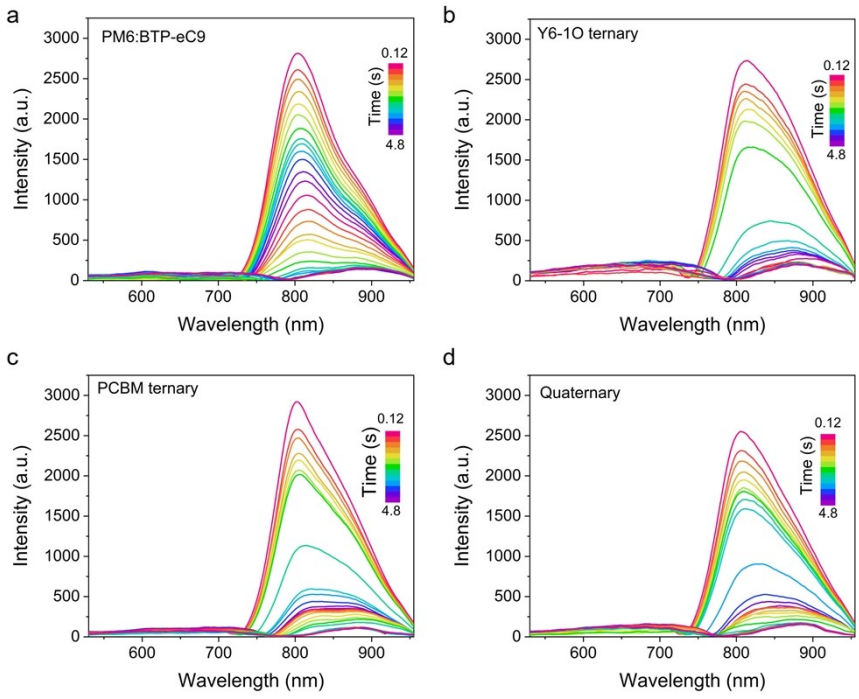

Figure S7. *In-situ* PL spectra of (a) PM6:BTP-eC9 (b) Y6-1O ternary (c) PCBM ternary and (d) quaternary blend films.

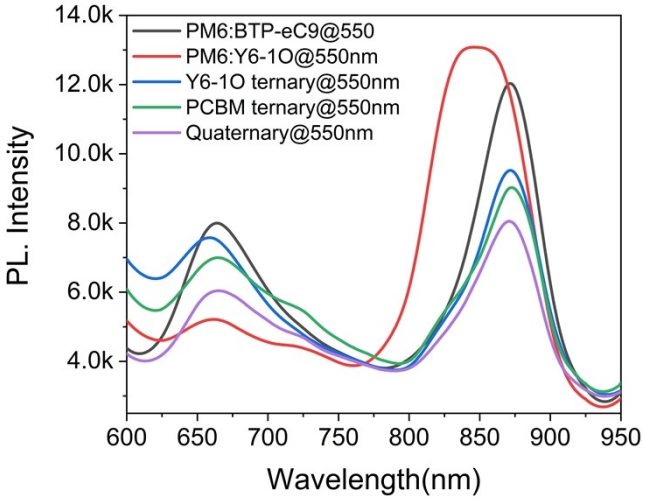

Figure S8. Steady-state PL spectra of PM6:BTP-eC9, PM6:Y6-1O, Y6-1O ternary, PCBM ternary and Quaternary blend films.

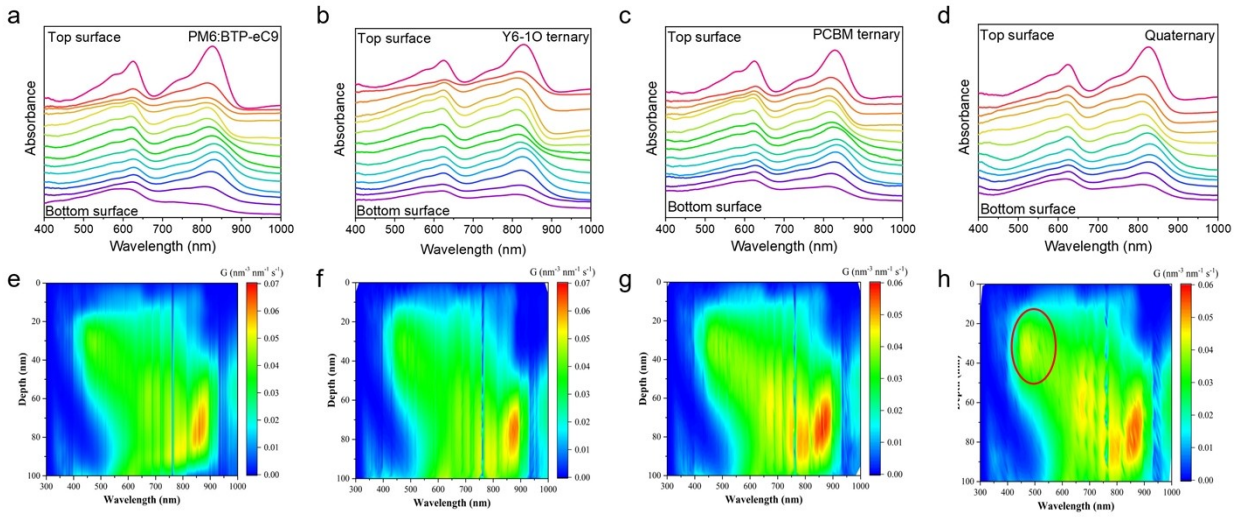

Figure S9. Film-depth-dependent phase segregation and exciton generation contours. (a-d) Film-depth-dependent light absorption spectra of 100 nm-thick (a) PM6:BTP-eC9 blend, (b) PM6:BTP-eC9:Y6-1O blend, (c) PM6:BTP-eC9:PCBM blend and (d) PM6:BTP-eC9:Y6-1O:PCBM blend. The spectra are vertically shifted for clarity, to show the optical properties at different film-depth. (e–h) Exciton generation contours of 100 nm-thick (e) PM6:BTP-eC9 blend, (f) PM6:BTP-eC9:Y6-1O blend:Y6-1O blend, (g) PM6:BTP-eC9:PCBM blend and (h) PM6:BTP-eC9:Y6-1O:PCBM blend, as simulated from spectra of (a-d) in combination with optical transfer-matrix approach. The noise-like vertical lines are due to features of the AM 1.5G solar spectra. 0 nm and 100 nm represent active layer/PNDIT-F3N and PEDOT:PSS/active layer interfaces, respectively. The incident light is from the bottom side.

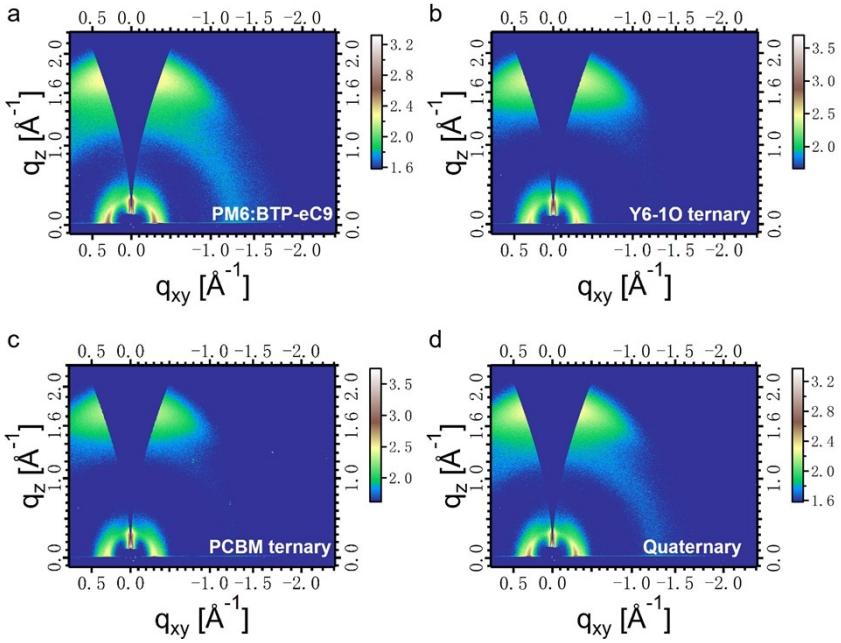

Figure S10. GIWAXS 2D maps of binary, ternary and quaternary blended films.

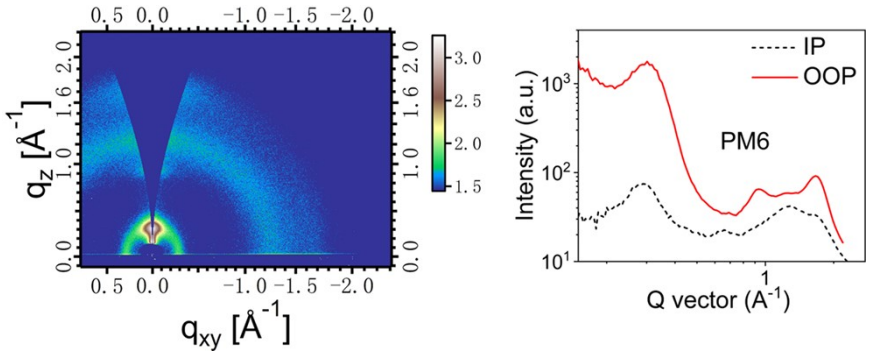

Figure S11. GIWAXS 2D maps and 1D profiles along the q_z direction of PM6 films.

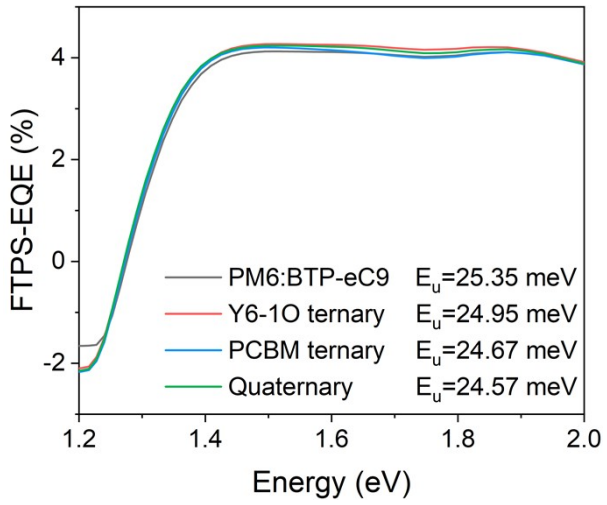

Figure S12. Highly sensitive EQE spectra of different OSC devices.

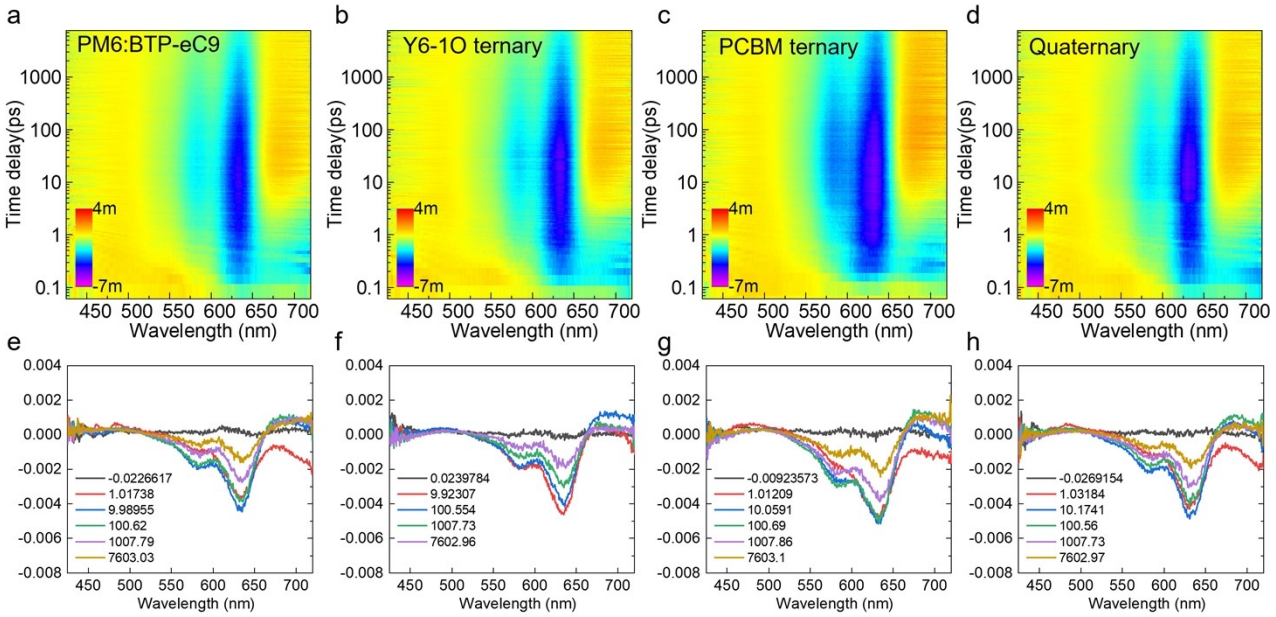

Figure S13. (a-d) Color plots of TA spectra of PM6:BTP-eC9, ternary and quaternary films under 800 nm excitation. TA spectra (e-h) in the range of 425–725 nm of the blends at different delay times.

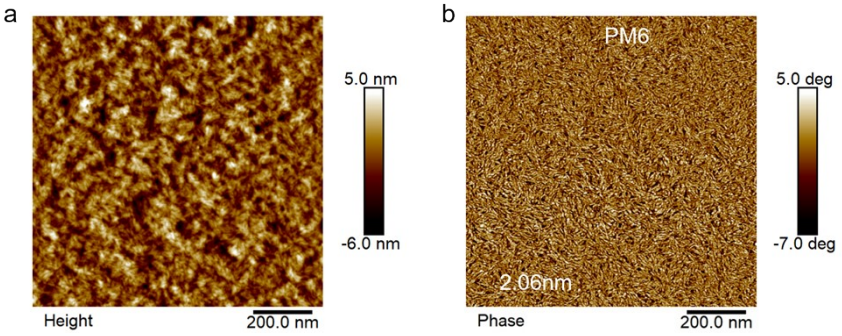

Figure S14. AFM (a) height and (b) phase image of PM6.

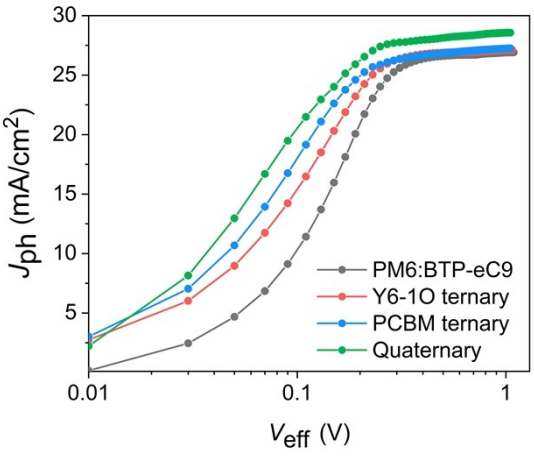

Figure S15. J_{ph} versus V_{eff} characteristics of the various blend systems.

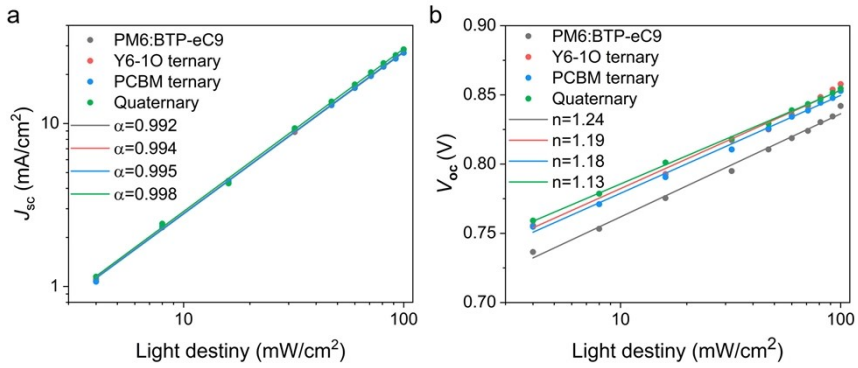

Figure S16. (a) Plots of J_{sc} versus light intensity and (b) V_{oc} versus light intensity for PM6:BTP-eC9 binary, Y6-1O ternary, PCBM ternary, and quaternary systems.

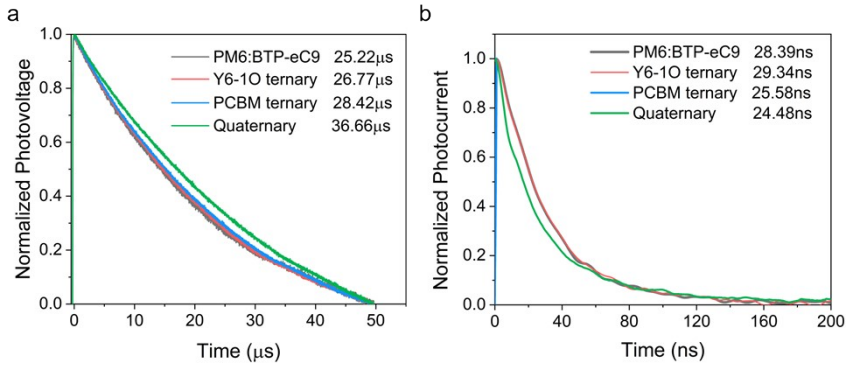

Fig. S17. Decay curves of (a) photovoltage and (b) photocurrent measured on various devices containing the photoactive layers of PM6:BTP-eC9, PM6:BTP-eC9:Y6-1O, PM6:BTP-eC9:$PC_{71}BM$, and PM6:BTP-eC9:Y6-1O:$PC_{71}BM$.

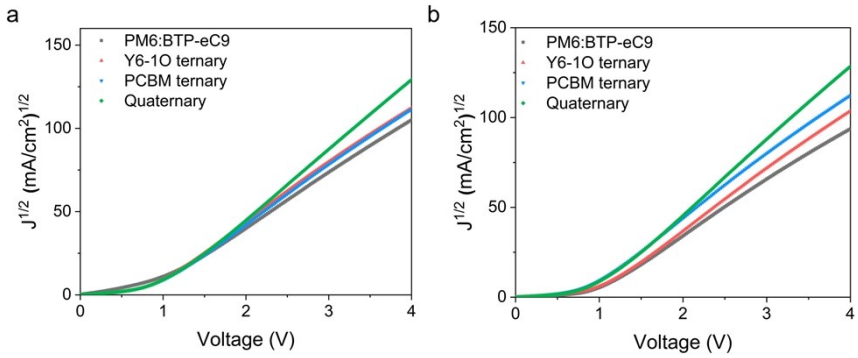

Figure S18. The $J^{0.5}$–V plots for determination of the electron (a) and hole (b) mobilities in various blends based on the space-charge-limited current (SCLC) method.

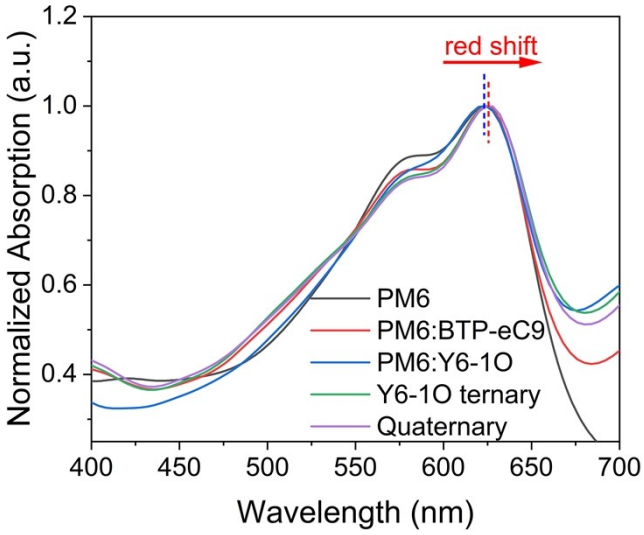

Figure S19. Thin-film absorption spectra of neat and blend films based on PM6, PM6:BTP-eC9, PM6:Y6-1O, PM6:BTP-eC9:Y6-1O and PM6:BTP-eC9:Y6-1O:$PC_{71}BM$.

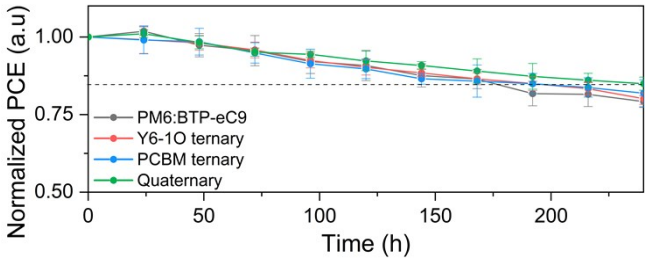

Figure S20. Normalized thermal stability of the devices in a nitrogen-filled glovebox at 60°C.

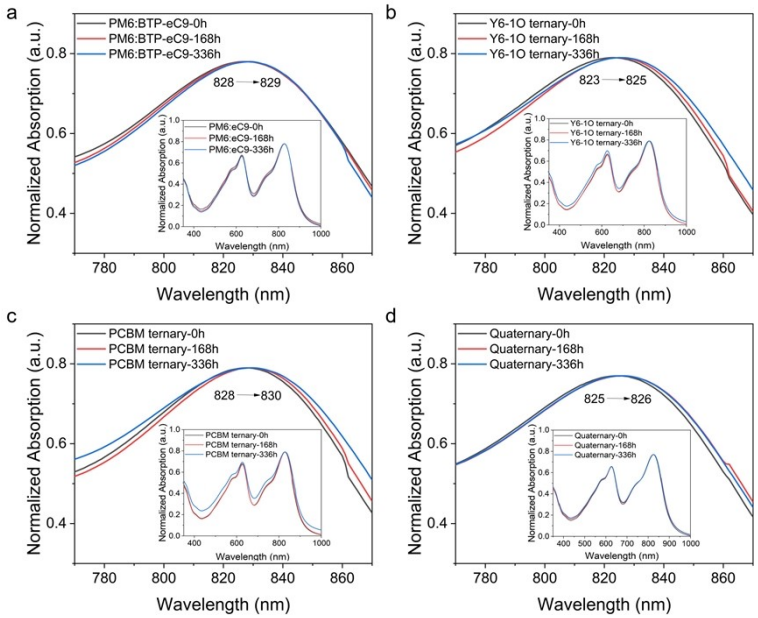

Figure S21. (a-d) Absorption spectra of various blend films measured before and after aging (under continuous AM 1.5 G illumination).

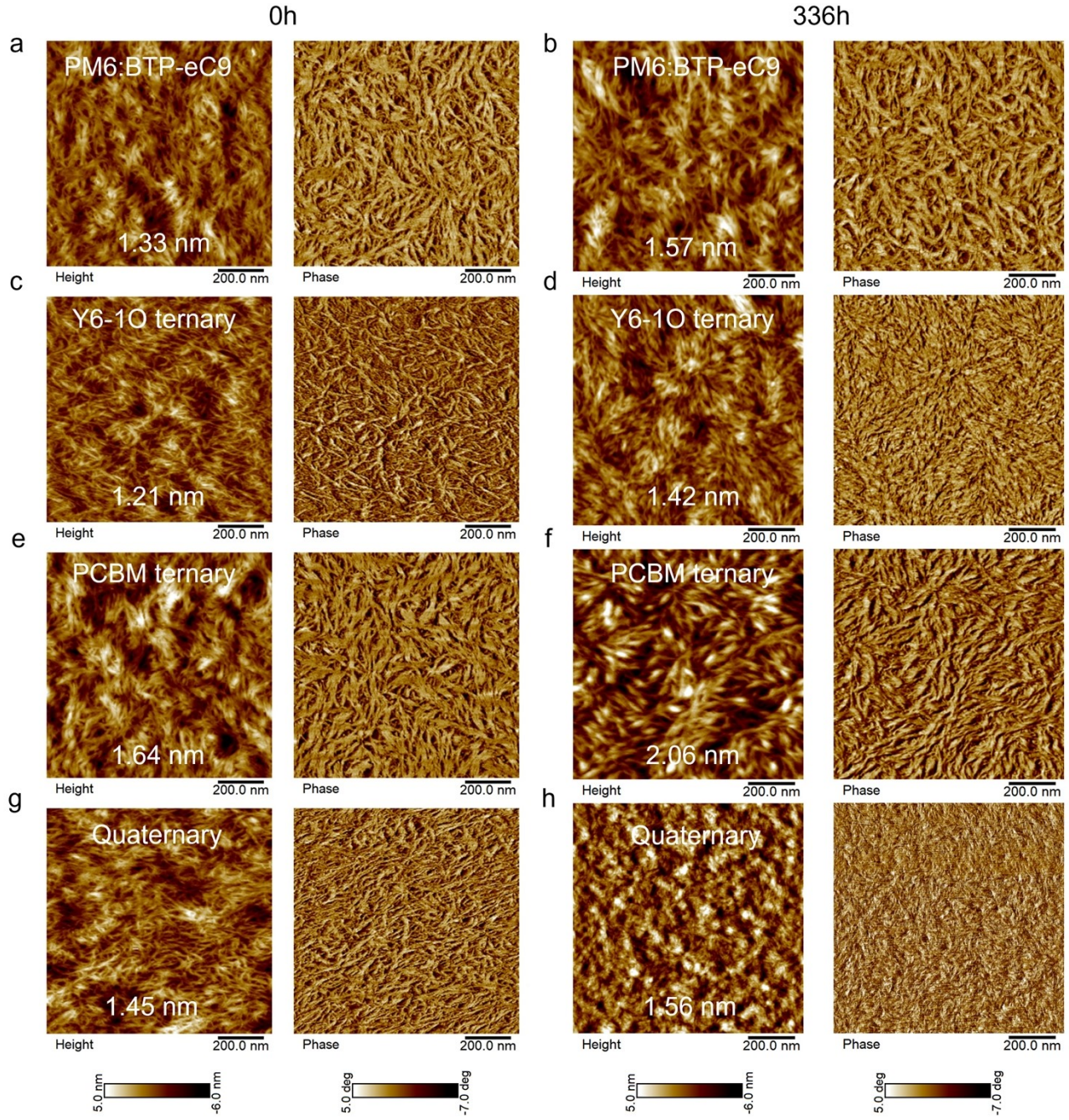

Figure S22. AFM height and phase images of (a, c, e, g) freshly prepared (0 h) and (b, d, f, h) aged (336 h) PM6:BTP-eC9, Y6-1O ternary, $PC_{71}BM$ ternary and quaternary blend films under continuous illumination (AM 1.5 G).

Table S1. The contact angles (θ), surface energy (γ), and Flory-Huggins interaction parameters ($\chi_{donor-acceptor}$) determined for BTP-eC9,Y6-1O,$PC_{71}BM$, BTP-eC9:Y6-1O and BTP-eC9:Y6-1O:$PC_{71}BM$ films.

Active layer	CA of water [deg.]	CA of Diiodomethane [deg.]	Surface energy [mN m^{-1}]	χ_{D-A} [K]
PM6	103.58	48.12	35.32	
BTP-eC9	100.29	37.18	40.99	0.211
Y6-1O	103.22	37.82	40.76	0.195
$PC_{71}BM$	89.13	25.62	46.49	0.766
BTP-eC9:Y6-1O	95.07	39.53	40.12	0.153
BTP-eC9:Y6-1O:$PC_{71}BM$	91.05	39.52	40.62	0.185

Table S2. Summary of the GIWAXS-relevant parameters of different blend films.

Active layer	Out-of-Plane	
	q ($Å^{-1}$)	CCL (Å)
PM6:BTP-eC9	1.63	13.18
Y6-1O ternary	1.74	12.07
$PC_{71}BM$ ternary	1.75	14.33
Quaternary	1.75	14.60

Table S3. Fitting parameters of TA dynamics (probed at 630 nm) of various blend films.

Active layer	630 nm		
	τ_1 (ps)	τ_2 (ps)	τ_3 (ps)
PM6:BTP-eC9	1.1	294	11580
Y6-1O ternary	1.3	239	12446
$PC_{71}BM$ ternary	3.9	311	10421
Quaternary	3.4	250	11035

Note: τ_1 is the rising edge

Table S4. Photocurrent data at different active layer ratios.

Active layer	V_{eff} [V] /$J_{ph, sat}$ [mA/cm^2]	V_{eff} [V] /$J_{ph, sc}$ [mA/cm^2]	V_{eff} [V] /J_{Mpp} [mA/cm^2]	$J_{ph, sc}$/ $J_{ph, sat}$	J_{MPP} / $J_{ph, sat}$
PM6:BTP-eC9	0.99/26.91	0.71/26.70	0.29/25.25	0.993	0.939
Y6-1O ternary	0.95/27.11	0.71/26.95	0.25/25.55	0.994	0.942
$PC_{71}BM$ ternary	0.93/27.81	0.71/27.07	0.13/25.25	0.995	0.943
Quaternary	0.93/28.53	0.71/28.36	0.23/27.05	0.995	0.948

Table S5. Charge carrier mobility in different blends determined with the SCLC method.

Active layer	μ_h (cm^2 V^{-1} s^{-1})	μ_e (cm^2 V^{-1} s^{-1})	μ_e/μ_h
PM6:BTP-eC9	4.42	5.03	1.14
Y6-1O ternary	4.48	5.41	1.20
$PC_{71}BM$ ternary	4.75	4.77	1.01
Quaternary	5.95	6.11	1.03

References

1. G. G. Malliaras, J. R. Salem, P. J. Brock and C. Scott, *Physical Review B*, 1998, **58**, R13411-R13414.
2. T.-Y. Chu and O.-K. Song, *Applied Physics Letters*, 2007, **90**.